A benchmark test system to assess angle stability in power systems with grid-forming power converters: Data

Régulo E. Ávila-Martínez[1,2], Javier Renedo[2], Luis Rouco[1,2], Aurelio Garcia-Cerrada[1,2], Lukas Sigrist[1,2]

[1] Instituto de Investigación Tecnológica (IIT), Madrid, Spain.
[2] ETSI ICAI, Universidad Pontificia Comillas, Madrid, Spain.

June 1, 2026

1 Introduction

This document describes the data of a benchmark test system to assess angle stability in power systems with grid-forming voltage source converters (GFM-VSC). This test system was used in [1].

The test system was developed in Matlab + Simulink + Simscape and it is suitable for ElectroMagnetic Transient (EMT) simulation, using example *power_PSS* of Simulink library [2] as a reference. Average EMT models of GFM-VSCs were considered, using and available models in open-source toolbox *VSC_Lib* [3–5]. Some of the GFM-VSC models were modified by the authors, in order to include specific controllers.

The objective of this test system is to analyse the ability of generators to remain in synchronism when subject to disturbances in power systems with both, synchronous machines (SM) and GFM-VSC power converters. The test system could be used to analyse small-disturbance and large-disturbance angle stability. Different parameters or operating conditions could be modified, in order to reproduce different kinds of instabilities or to test mitigation measures.

2 Benchmark test system

Fig. 1 shows the test system, which consists of a synchronous machine (SM-1) and a grid-forming power converter (GFM-VSC-2) connected to an infinite grid through transmission lines. The system consists of Area A of the well-known Kundur's two-area system [6, 7], with an infinite grid connected at bus 6. A GFM-VSC is connected at bus 2, instead of the synchronous machine of the original system. Nominal voltage and frequency of the system are 220 kV and 50 Hz, respectively.

Table 1 depicts the line data (base values for pu: 220 kV and 100 MVA). Load L_5 is consuming 967 MW and 100 MVAr in the initial operating point and it is modelled as a constant impedance for dynamic simulations. The rating of the shunt capacitor bank connected at bus 5 is 200 MVAr. Sections 3 and 4 describe the dynamic models and data of synchronous machine SM-1 and of grid-forming power converter GFM-VSC-2, respectively.

Table 1: Test system. Line data. Base for pu: 100 MVA and 220 kV.

Line	$r_{s,ij}$ (pu)	$x_{s,ij}$ (pu)	$b_{p,ij}$ (pu)
3-4	0.0025	0.0250	0.0438
4-5	0.0010	0.0100	0.0175
5-6a	0.0165	0.1650	0.2888
5-6b	0.0165	0.1650	0.2888

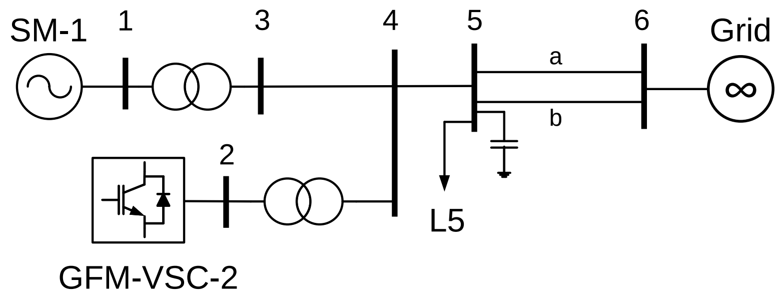

Figure 1: Test system.

Two case studies were analysed in [1]:

- Study 1: Large-disturbance angle stability: Case A (second column of Table 2).
- Study 2: Small-disturbance angle stability:
  - Stable case: Case A (second column of Table 2). This one is the same case than the one used in Study 1 (large-disturbance angle stability).
  - Stable case: Case B (third column of Table 2). In this case, some modifications were made, in order to obtain a critical scenario in terms of oscillatory stability: the active-power injection at the initial operating point of generators SM-1 and GFM-VSC-2 were increased ($P_{g,1}^0 = P_{g,2}^0 = 700$ MW), the Power System Stabilizer (PSS) of SM-1 was disabled and the damping coefficient of GFM-VSC-2 was reduced from $D_{GFM} = 193$ pu to $D_{GFM} = 20$ pu (see Fig. 6 of Section 4). See sections 3 and 4 for all details of the parameters of the dynamic models of the generators.

Table 2: Cases A and B.

Bus	Case A	Case B
SM-1	$P_{g,1}^0 = 600$ MW, $v_1^0 = 1$ pu.	$P_{g,1}^0 = 700$ MW, $v_1^0 = 1$ pu.
GFM-VSC-2	$P_{g,2}^0 = 600$ MW, $e_{m,2}^0 = 1.0475$ pu.	$P_{g,2}^0 = 700$ MW, $e_{m,2}^0 = 1.0498$ pu.
Infinite grid (G6)	$v_6^0 = 1$ pu, $\theta_6^0 = 0º$ (slack).	$v_6^0 = 1$ pu, $\theta_6^0 = 0º$ (slack).

3 Synchronous machine

Synchronous generator and transformer nameplate (SM-1):

- Synchronous machine: 900 MVA, 20 kV, 50 Hz, pole pairs: 4.
- Transformer: 900 MVA, 220/20 kV, $r_{cc} = 0$ pu, $x_{cc} = 0.15$ pu.

Dynamic models of the synchronous generator:

- Synchronous machine: GENROU model [8], with parameters: $H = 6.5$ s, $D = 0$ pu, $X_d = 1.8$ pu, $X'_d = 0.3$ pu, $X''_d = X''_q = 0.25$ pu, $X_q = 1.7$ pu, $X'_q = 0.55$ pu, $X_l = 0.2$ pu, $T'_{do} = 8$ s, $T''_{do} = 0.03$ s, $T'_{qo} = 0.4$ s, $T''_{qo} = 0.05$ s, $R_s = 0.0025$ pu.
- Turbine and speed regulator (governor): Steam turbine with model STG [2]. Parameters: $K_p = 1$ pu, $R_p = 0.05$ pu, $D_z = 0$ pu, $T_{sr} = 0.001$ s, $T_{sm} = 0.15$ s, $v_{gmin} = -0.1$ pu, $v_{gmax} = 0.1$ pu/s, $g_{min} = 0$ pu, $g_{max} = 4.496$ pu, $T_2 = 0$ s, $T_3 = 10$ s, $T_4 = 3.3$ s, $T_5 = 0.5$ s, $F2 = 0$, $F3 = 0.36$, $F4 = 0.36$, $F5 = 0.28$.
- Excitation system and automatic voltage regulator (AVR): Model ST1C (Fig. 2 [9]), with parameters: $K_A = 200$ pu, $T_A = 0.001$ s, $T_R = 0.02$ pu, $V_{Rmax} = 12.3$ pu, $V_{Rmin} = 0$ pu, $V_{Amax} = 12.3$ pu, $V_{Amin} = 0$ pu, $R_C = 0$ pu, $X_C = 0$ pu, $T_B = 0$ s, $T_C = 0$ s, $T_{B1} = 0$ s, $T_{C1} = 0$ s, $V_{Imax} = 99$ pu, $V_{Imin} = -99$ pu, $K_F = 0$ pu, $T_F = 1$ s, $K_C = 0$ pu, $K_{LR} = 0$ pu, $I_{LR} = 0$ pu.
- Power system stabiliser (PSS): Single-input PSS with model PSS1C (Fig. 3 [9]), using as input signal the speed deviation $\Delta\omega$ and parameters: $K_S = 30$ pu, $T_5 = 10$ s, $T_1 = 0.05$ s, $T_2 = 0.02$ s, $T_3 = 3$ s, $T_4 = 5.4$ s, $T_6 = 0$ s, $A_1 = A_2 = 0$, $V_{STmax} = 0.15$ pu, $V_{STmin} = -0.15$ pu.

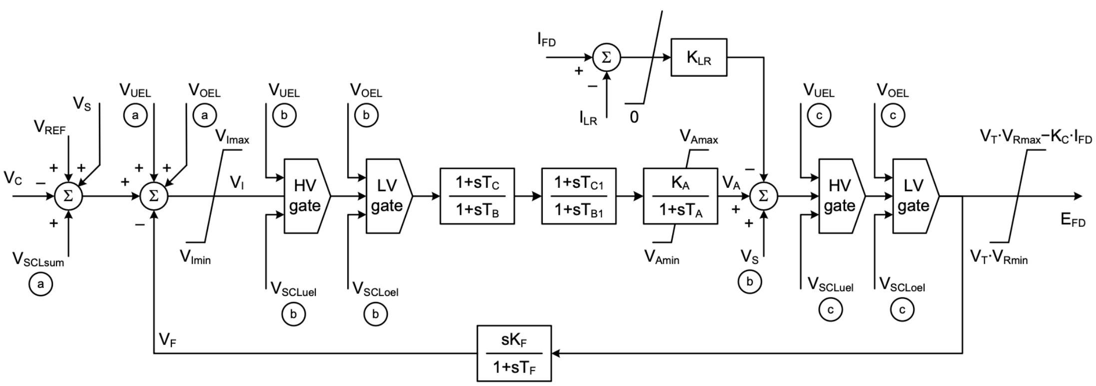

Figure 2: Excitation system type ST1C. Figure from [9].

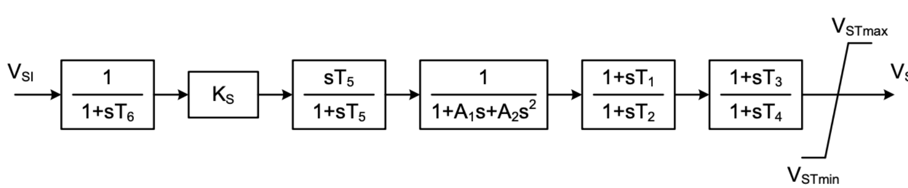

Figure 3: PSS type PSS1C. Figure from [9].

4 GFM-VSC power converter

Fig. 4 shows the scheme of GFM-VSC-2, where $\bar{e}_m$ is the modulated voltage of the GFM-VSC, and $\bar{z}_c = r_c + jx_c$ ($x_c = L_c\omega$) is the series impedance (equivalent series reactor and the impedance of the transformer), $\bar{v}_g$ is the AC voltage at the connection point, $\bar{i}_g$ is the current injection of the GFM-VSC, and p_g and q_g are its active- and reactive-power injections, respectively.

Main control aspects of the GFM-VSC power converter can be summarised as follows:

- Control system of the GFM-VSC (Fig. 5), which follows the control scheme used in [10, 11] (current-controlled GFM-VSC). The current controller has a limiter based on Current Saturation Algorithm (CSA) [12], with equal priority for d- and q-axis currents.
- GFM-VSC self-synchronisation strategy, based on Virtual Synchronous Machine (VSM) with frequency estimation at the connection point via a phase-locked loop (VSM-PLL, for short), following the approach of [13] (Fig. 6). The design of the parameters of VSM-PLL control strategy was carried out as in [14].
- Table 3 shows the data of the GFM-VSC.

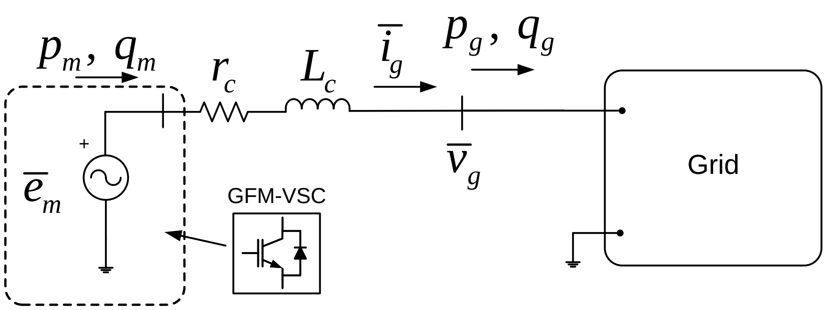

Figure 4: Equivalent model of the GFM-VSC connected to the grid.

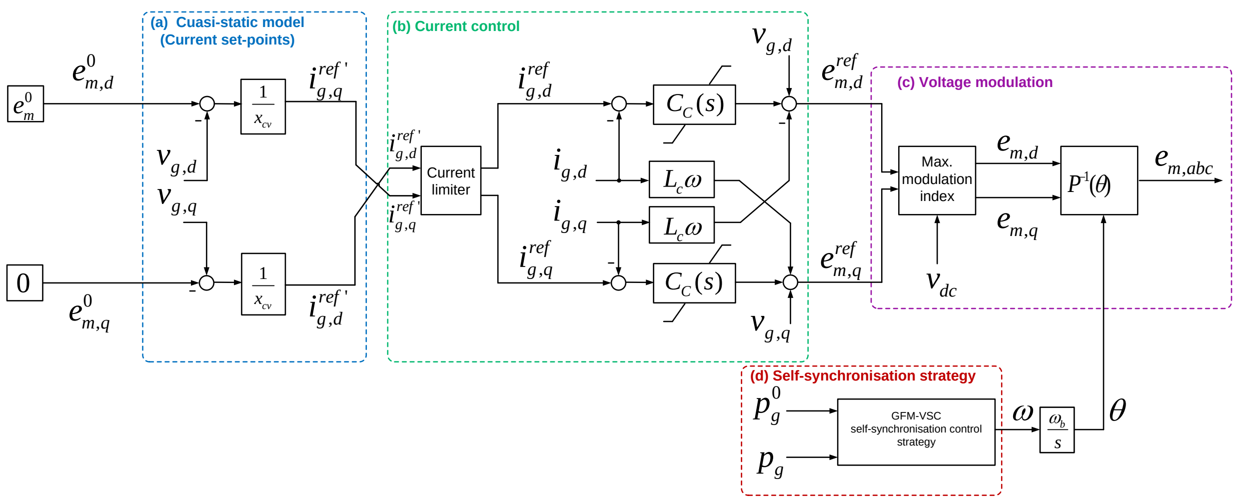

Figure 5: Control system of the GFM-VSC.

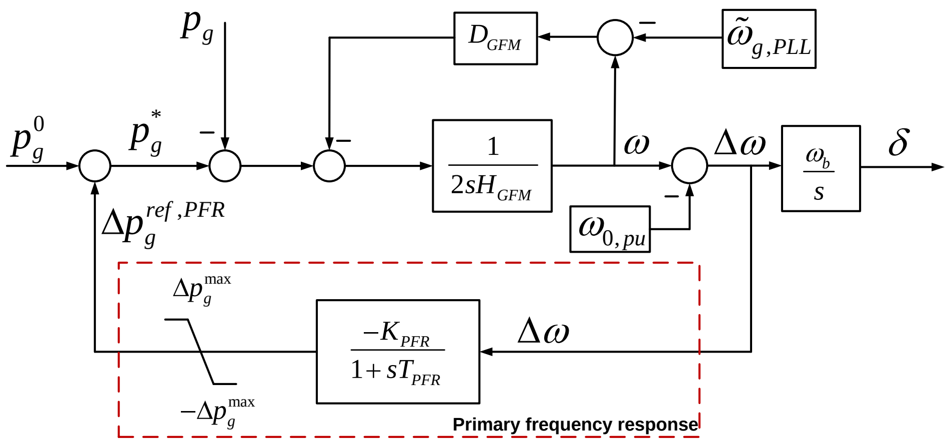

Figure 6: GFM-VSC self-synchronisation strategy.

Table 3: Parameters of the GFM-VSC.

Parameters GFM-VSC's rating are base values for pu	**Values**
Rating VSC, DC voltage, AC voltage	900 MVA, 640 kV, 320 kV
Max. current	1.20 pu (equal priority for $d-q$ axes)
Series resistance ($r_{c,i}$) / reactance ($x_{c,i}$) (equivalent inductance + transformer) (transformer: 900 MVA 220/320 kV)	0.005 pu / 0.15 pu
Current control bandwidth ($\omega_{n,CC}$)	1500 rad/s
Current control prop. / int. gains ($K_{C,P,i}$ / $K_{C,I,i}$)	1.0027 pu / 1074.3 pu/s
Quasi-static model, virt. reactance (x_v / x_{ev})	0 pu / 0.15 pu
Emulated inertia ($H_{GFM,i}$)	4.5 s
Primary freq. controller ($K_{PFR,i}$ / $T_{PFR,i}$)	20 pu / 1 s
Primary freq. controller limit ($\Delta p_{g,i}^{max}$)	1 pu
PLL control bandwidth ($\omega_{n,PLL}$)	500 rad/s
PLL control porp. / int. gains ($K_{P,PLL}/K_{I,PLL}$)	3.18 pu / 795.77 pu/s
PLL frequency saturation ($\Delta\omega_{PLL}^{max}$)	± 0.1 pu

Acknowledgements

Work supported by the Spanish Government under a research project ref. PRE2019-088084, RETOS Project Ref. RTI2018-098865-B-C31 (MCI/AEI/FEDER, UE) and Project PID2021-125628OB-C21 (MICIU/AEI /10.13039/501100011033 and FEDER, EU); and by Madrid Regional Government under PROMINT-CM Project Ref. S2018/EMT-4366. Internal reference of this document: IIT-25-372WP.

Contact: {regulo.avila, luis.rouco, aurelio, lukas.sigrist}@iit.comillas.edu, javier.renedo@ieee.org.

References

[1] R. E. Ávila-Martínez, J. Renedo, L. Rouco, A. Garcia-Cerrada, and L. Sigrist, "Revisiting angle stability in power systems with grid-forming power converters," *arXiv preprint*, no. arXiv:2605.19380, doi: doi.org/10.48550/arXiv.2605.19380, pp. 1–4, 2026.

[2] Mathworks, "power_pss system," vol. www.mathworks.com (accessed 17-12-2025), 2025.

[3] L2EP-LILLE, "VSC_lib: Grid forming models for Matlab/SimPowerSystem," vol. https://github.com/l2ep-epmlab/ (accessed 08-07-2020), 2020.

[4] T. Qoria, Q. Cossart, C. Li, X. Guillaud, F. Colas, F. Gruson, and X. Kestelyn, "WP3-Control and Operation of a Grid with 100% Converter-Based Devices. Deliverable 3.2: Local control and simulation tools for large transmission systems," MIGRATE Project, Tech. Rep., 2018.

[5] T. Qoria, F. Gruson, F. Colas, G. Denis, T. Prevost, and X. Guillaud, "Inertia effect and load sharing capability of grid forming converters connected to a transmission grid," in *Proc. 15th IET Int. Conf. on AC and DC power transmission (ACDC), Coventry, UK*, 2019, pp. 1–6.

[6] M. Klein, G. J. Rogers, and P. Kundur, "A Fundamental Study of Inter-Area Oscillations in Power Systems," *IEEE Transactions on Power Systems*, vol. 6, no. 3, pp. 914–921, 1991.

[7] P. Kundur, *Power system stability and control.* McGraw Hill Education, New York, NY, USA, 1994.

[8] Siemens PTI, "PSS/E 35.3.2: Model Library," User manual, Schenectady, NY, USA, Tech. Rep., 2021.

[9] IEEE, "IEEE Std 421.5-2016: IEEE Recommended Practice for Excitation System Models for Power System Stability Studies," IEEE, New York, NY, USA, Tech. Rep., 2016.

[10] K. Vatta Kkuni, S. Mohan, G. Yang, and W. Xu, "Comparative assessment of typical control realizations of grid forming converters based on their voltage source behaviour," *Energy Reports*, vol. 9, pp. 6042–6062, Dec. 2023.

[11] Y. Laba, A. Bruyère, F. Colas, and X. Guillaud, "Virtual Power-Based Technique for Enhancing the Large Voltage Disturbance Stability of HV Grid-Forming Converters," in *2023 25th European Conference on Power Electronics and Applications (EPE'23 ECCE Europe).* Aalborg, Denmark: IEEE, Sep. 2023, pp. 1–8.

[12] T. Qoria, F. Gruson, F. Colas, X. Kestelyn, and X. Guillaud, "Current limiting algorithms and transient stability analysis of grid-forming VSCs," *Electric Power Systems Research*, vol. 189, no. 106726, pp. 1–8, 2020.

[13] S. D'Arco, J. A. Suul, and O. B. Fosso, "A Virtual Synchronous Machine implementation for distributed control of power converters in SmartGrids," *Electric Power Systems Research*, vol. 122, pp. 180–197, 2015.

[14] R. E. Ávila Martínez, X. Guillaud, J. Renedo, L. Rouco, A. Garcia-Cerrada, and L. Sigrist, "Impact on transient stability of self-synchronisation control strategies in grid-forming power converters," *International Journal of Electrical Power & Energy Systems*, vol. 174, no. 111540, pp. 1 – 18, 2026.